Article

pubs.acs.org/Biomac

Peptide Self-Assembly on Cell Membranes to Induce Cell Lysis

Long Chen, Nicole Patrone, and Jun F. Liang*

Department of Chemistry, Chemical Biology, and Biomedical Engineering, Charles V. Schaefer School of Engineering and Sciences, Stevens Institute of Technology, Hoboken, New Jersey 07030, United States

ABSTRACT: Self-assembling into aggregates with defined structures is a common phenomenon for many peptides at high concentrations. In this study, we found that when PTP-7b (FLGALFKALSHLL), a concentration-dependent self-assembling peptide, bound to tissue cells and accumulated on cell surfaces, it migrated and self-assembled into exosome-like aggregates at certain locations on the cell membranes. Studies using confocal microscopy and scanning electron microscopy revealed that peptide PTP-7b induced cell tissue damage through a new cell lysis mechanism that involved peptide self-assembly on cell surfaces, extracting lipids from cell membranes, and transporting peptides into the cytoplasm. Peptide self-assembly attributed greatly to peptide-cell interactions and thus the biological activity of a peptide. Because peptide self-assembly was a slow process, PTP-7b-induced cell lysis showed a biphasic behavior: a gradual viability decrease was followed by a rapid decline. These results suggest that peptide self-assembly could be equally as important as charge and secondary structure of a peptide in determining the anticancer and antibacterial activities of therapeutic peptides.

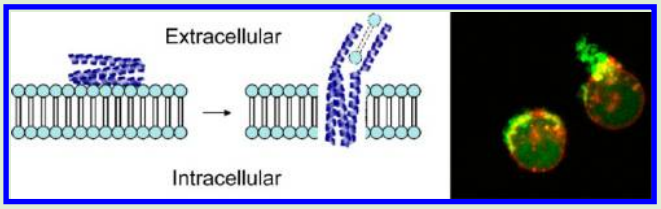

INTRODUCTION

Therapeutic peptides are a group of peptides that have defined biological activities and are used for the treatment of various diseases including autoimmune diseases, infections, and cancers.[1,2] Traditionally, therapeutic peptides have been derived from natural or bioactive peptides produced by plants, animals, or humans with a length of up to 50 amino acids. Among all therapeutic peptides, the interaction of membrane-acting (lytic) peptides with the lipid bilayer of cells has been well studied.[3−5] Three different models, barrel-stave, toroidal, and carpet model, are used to describe the acting mechanisms of most cationic antimicrobial and anticancer peptides.[6,7] Both the barrel-stave model and the toroidal model are pore formation models.[5] In the barrel stave model, peptides insert into the membrane bilayer and form the pore by themselves. However, in the toroidal model, the peptide interacts with the membrane lipid headgroups, and the membrane pores are formed by the peptide and lipid molecules. In the carpet model, the peptides disrupt the membrane by orienting parallel to the surface of the lipid bilayer and forming an extensive layer or carpet.[6] At high peptide concentrations, peptides disrupt the bilayer in a detergent-like manner, eventually leading to the formation of micelles.

Despite different models, interactions of membrane-acting peptides with the lipid bilayer of cell membranes have a common feature and can be divided into three thermodynamic steps: (1) the electrostatic attraction of cationic peptides to anionic cell membranes; (2) the transition of the peptide into the plane of binding and accumulation on the surfaces of cell membranes; and (3) the insertion of concentrated peptides into cell membranes to induce cell lysis.[8] The electrostatic attraction of cationic peptides to the cell membranes is the critical step, which is solely determined by the net positive charges of a peptide.[9] This is the reason why all lytic peptides are positively charged with very few exceptions. In addition, the folding of the peptide chain into a specific conformation, usually an α-helical structure, has proven to be a necessary and energy favorable process for peptide insertion into cell membranes.[10]

Self-assembling into aggregates in solutions with defined structure is a common phenomenon for many therapeutic peptides.[15−17] The results from our studies on peptide aggregation suggest that peptides may never exist as a single molecule in solutions.[10] Depending on their charges, sequences, secondary structures, and solvation properties, therapeutic peptides may self-assemble into huge peptide aggregates with defined nanostructures. This is especially true at high peptide concentrations. Since the result of a peptide binding to cells is several hundred times concentrated on cell membranes,[19] it is reasonable to believe that peptide self-assembly may also happen on cell membranes.

In this study, we reported that peptide self-assembled on cell membranes into exosome-like aggregates and induced cell lysis through a new mechanism. The results from this study prove that peptide self-assembly might be equally as important as the charges and secondary structures of peptides and contribute greatly to the biological activity of therapeutic peptides.

MATERIALS AND METHODS

Materials. A LIVE/DEAD bacteria staining kit was purchased from Invitrogen Life Technologies (Carlsbad, CA). Peptides were synthesized by GenScript (Piscataway, NJ). The purity (>90%) of

Received: July 16, 2012
Revised: August 19, 2012
Published: August 30, 2012

the peptide was analyzed by HPLC and electrospray ionization mass spectrometry. The human lung carcinoma cell line A549 was obtained from American Type Culture Collection (ATCC, Manassas, VA). All other reagents, if not mentioned, were from Sigma Chemical Laboratory (St Louis, MO).

Methods. *Peptide Aggregate Measurement and Characterization.* Peptides from stock solutions (5 mM in water/DMSO mixture) were diluted with PBS of various pHs. Peptide solutions were incubated at 37 °C for 24 h to allow the formation of dynamically stable peptide aggregates. The sizes of peptide aggregates in solutions were measured using a Zeta nanosizer. Morphologies of peptide aggregates were studied using scanning electron microscopy (SEM) as described in previous studies.[10]

Kinetic Studies of Peptide-Induced Cell Membrane Damage Using a LIVE/DEAD Kit. Freshly trypsinized human lung carcinoma A549 cells were seeded in a collagen-coated 8-well glass chamber (2×10^4 cells/well) and cultured in F12K medium containing 10% fetal bovine serum (FBS) at 37 °C (5% CO_2) overnight. Before the assay, cells were washed with phosphate-buffered saline (PBS) three times and stained with the LIVE/DEAD staining kit for 15 min. After the addition of peptides, cell images were recorded at different time points using a Zeiss LSM510 Confocal Microscope. The excitation wavelength was fixed at 488 nm, and the emission wavelengths were set at 505−530 nm (for the live cells) and 560 nm (for the dead cells). The percentage of green pixels out of total green and red pixels in captured cell images was calculated to estimate the cell membrane integrity.

Cell Lysis Assay Using a Lactate Dehydrogenase Kit. Overnight cultured A549 cells on 96-well plates (5×10^3 cells/well) were washed with PBS three times before they were exposed to peptides. Peptide-caused cell membrane damage was quantitatively assessed by measuring lactate dehydrogenase (LDH) release from damaged cells after 20 and 60 min of incubation using the LDH kit according to the protocol provided by the manufacturer. The absorbance at 490 nm was measured using a Biotek microplate reader by setting a reference wavelength at 690 nm. Results were normalized to cell death percentage against both blank and 100% lysis controls.

End-Point Cytotoxicity Assay Using MTT. The cytotoxicity of the peptides was determined using the MTT assay as described previously.[14] Briefly, cells in a complete medium were added into 96-well plates (5×10^3 cells/well) and cultured at 37 °C for 14−16 h. After being washed, cells were fed with serum-free F12K medium containing various concentrations of peptides and incubated at 37 °C for 2 h. After that, 10 μL of MTT (5 mg/mL) were added into each well. Cell viability was determined after 4 h of incubation by dissolving crystallized MTT with 10% SDS solution containing 5% isopropanol and 0.1% HCl and measuring absorbance at 570 nm.

Study of Peptide-Cell Membrane Interaction Using Confocal Microscopy. Freshly trypsinized human lung carcinoma A549 cells were seeded in a collagen-coated eight-well glass chamber (2×10^4 cells/well) and cultured in F12K medium containing 10% FBS at 37 °C (5% CO_2) overnight. Before the assay, cell membranes were stained with Di-8-ANEPPS (2.5 μM) for 10 min. After being washed three times with PBS to remove excess Di-8-ANEPPS, cells were exposed to fluorescein isothiocyanate (FITC)-labeled peptides. Peptide accumulation and self-assembly on cell surfaces were investigated using the Zeiss LSM510 Confocal Microscope by setting the excitation wavelength at 488 nm and emission wavelength at 505−530 nm (for peptides) and 560 nm (for cell membranes), respectively.

SEM Analysis of Peptide-Treated Cells. A549 cells were seeded on pieces (1.5 × 1.5 cm) of silicon wafer and cultured in a six-well plate overnight. Cells on silicon wafers were washed with PBS and then treated with peptides for 30 min. After that, cells were fixed with 2% paraformaldehyde and washed with ethanol with gradually increased concentrations (5% to 99%). Fixed cell samples were then coated with gold for SEM analysis. SEM images of cells were taken using an Auriga Modular CrossBeam workstation (Carl Zeiss, Inc.) operating at 5 kV.

Measurement of Peptide-Induced Transmembrane Potential Changes in Cells. Freshly trypsinized A549 cells were suspended in Tyrode's solution (137 mM NaCl, 5.4 mM KCl, 0.5 mM $MgCl_2$, 11.6 mM HEPES, 1.8 mM $CaCl_2$, 10 mM glucose, pH was adjusted to 7.4) at 10^7 cells/ml. Cells were treated with 5 μM DiSC3(5) at 37 °C for 10 min. Peptide-induced fluorescence intensity change in cells was recorded at intervals of 15 s (excitation wavelengths = 650 nm; emission wavelengths = 675 nm) using a Biotek Synergy MX fluorescence microplate reader.

RESULTS AND DISCUSSIONS

Peptides with specific sequences can self-assemble into aggregates with regular structures.[11,12] An obvious example of self-assembly is β-amyloid, in which peptides of about 40 amino acids in length can self-assemble into insoluble fibrous peptide aggregates to cause various neurodegenerative disorders.[13] We had used lytic peptide PTP-7 (FLGALFKALSKLL) as a template to construct two peptide derivatives (PTP-7a, FLGALFHALSKLL, PTP-7b, FLGALFKALSHLL) with the same amino acid composition but having the only histidine residue at different positions (position #7 for PTP-7a and position #11 for PTP-7b). Although peptide PTP-7 and its two derivatives were able to self-assemble into amyloid-like structures,[10] only PTP-7b formed large (>1.0 μm) and dynamically stable aggregates after long incubations (Figure 1).

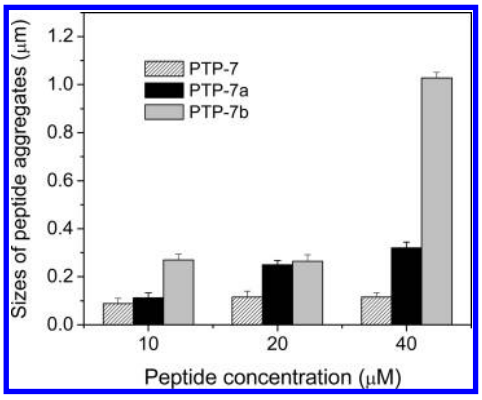

Figure 1. Particle sizes of formed peptide aggregates in the solution. Peptide solutions of various concentrations were stabilized at 37 °C for 24 h, and then the particle sizes were measured by a Zeta nanosizer. Data represents the mean and SD of three independent tests.

The results from the SEM study revealed that, unlike PTP-7 aggregates having fibril-like structures, big PTP-7b aggregates were assembled from many round units of 10−20 nm in size (Figure 2). It should be pointed out that due to the presence of solvation, measured aggregate sizes in solutions using nanosizer were much bigger (1100 nm) than what was observed under SEM (average = 420 nm). Even more interestingly, PTP-7b showed a good aggregation-concentration correlation and could form peptide aggregates at low peptide concentrations (40 μM) (Figure 1).

We reported that PTP-7b and PTP-7a were less (~3 times) active than PTP-7 because of altered peptide solvation and reduced membrane binding ability in these two peptides.[10] PTP-7a and PTP-7b demonstrated almost the same cell lysis ability, as determined using the end point MTT assay.[10] However, dynamic studies of cell membrane lysis using LIVE/DEAD dye staining revealed that PTP-7b induced cell lysis through a different mechanism from PTP-7 and PTP-7a. Peptide PTP-7b-induced cell death was a biphasic process: a gradual viability decrease followed by a sudden cell lysis (Figure 3). Although the cell lysis capability of PTP-7b was concentration dependent, PTP-7b at different concentrations

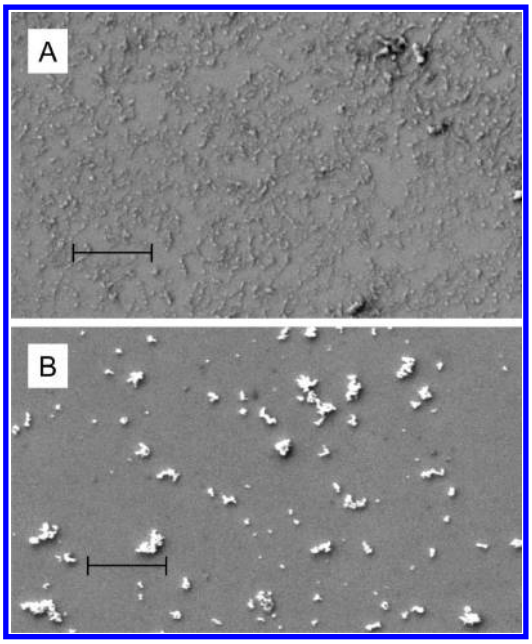

Figure 2. SEM images of peptide PTP-7 (A) and PTP-7b (B). Peptides (40 μM in water) were incubated at 37 °C for 24 h. The solutions were deposited onto a piece of silicon wafer for 10 min and washed with deionized water to remove the salts. Samples were coated with gold before taking the SEM images. Scale bar = 1.0 μm.

had nearly the same transition point at around 60 min. Therefore, despite the comparable cytotoxic activity of PTP-7a and PTP-7b (the IC_{50} were at 28 and 32 μM for PTP-7a and PTP-7b on A549 cells as measured using end-point MTT assay), the rapid cell lysis phase made PTP-7b much more powerful than PTP-7a in inducing cell membrane damage (Figure 3).

The acting mechanism change of PTP-7b over the course of incubation was confirmed in another membrane lysis assay by comparing peptide-induced LDH release. As shown in Figure 4, although PTP-7a and PTP-7b had very close cell lysis activity at the early phase (20 min) of incubation, peptide PTP-7b surpassed PTP-7a and demonstrated extremely strong cell lysis ability after the incubation passed the transition time point (~60 min). This is consistent with the results from the membrane integrity assay (Figure 3) and confirms the biphasic cell killing mechanism of peptide PTP-7b.

To further understand the acting mechanism of PTP-7b, interactions between PTP-7b and cells were studied using FITC-labeled peptides and Di-8-ANEPPS-labeled cell membranes. Since PTP-7 was much more potent and caused complete cell lysis within a very short incubation time (30 min), for better comparison of the dynamic processes of these two induced cell lysis, different concentrations of PTP-7 (10 μM) and PTP-7b (40 μM) were used in this study.

Peptide PTP-7 damaged the cell membranes by forming an extensive layer on cell surfaces and disrupting the lipid bilayer of cells in a detergent-like manner, leading to the formation of lipid micelles (Figure 5A–C). Severely damaged cell membranes were observed after 30 min incubation. Although PTP-7b also formed an extensive layer on cell surfaces at the beginning (<30 min) of incubation (Figure 5D), membrane bound PTP-7b was quickly concentrated at a few locations on cell membranes and formed peptide aggregates there. As the incubation time increased, the peptide aggregates on cell

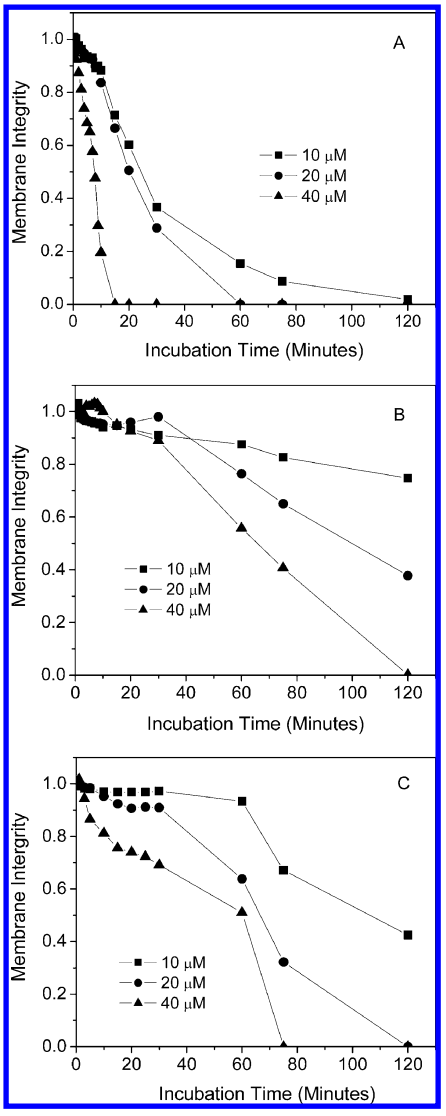

Figure 3. Dynamics of peptide PTP-7 (A), PTP-7a (B), and PTP-7b (C) induced cell membrane permeation to LIVE/DEAD dyes. Fluorescence images were taken after peptide solutions were added at different time points. The percentage of green pixels out of the total green and red pixels was calculated to estimate the cell membrane integrity.

membranes became more significant. Obvious intracellular translocation and cytoplasm accumulation of PTP-7b was observed after 60 min of incubation even though cells maintained nearly intact cell membranes at this time point (Figure 5E). After this point, cell membrane damage occurred at PTP-7b aggregate locations as a result of lipid migration from cell membranes into PTP-7b aggregates on cell surfaces, indicated by an obvious color change of peptide aggregate from green (FITC-labeled peptides) to yellow (a mixture of FITC-labeled peptides and Di-8-ANEPPS labeled lipids) (Figure 5F).

The difference between PTP-7- and PTP-7b-induced cell membrane damage was compared further at the time point of cell lysis using the same concentration (40 μM) of peptides (Figure 6). Severely disrupted cell membranes and the formation of lipid vesicles by released lipids from damaged cell membranes were clearly seen in PTP-7-treated cells. By contrast, in the PTP-7b treated cells, disrupted cell membranes were only observed at the locations of peptide aggregates when

dx.doi.org/10.1021/bm301106p | *Biomacromolecules* 2012, 13, 3327–3333

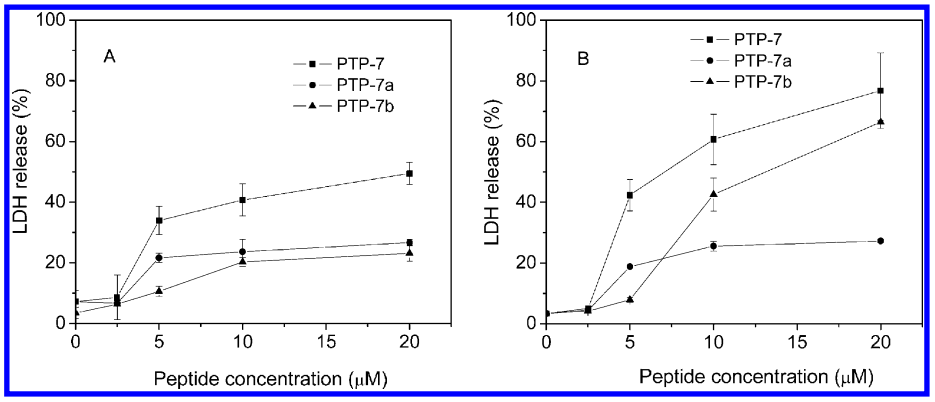

Figure 4. Comparison of PTP-7-, PTP-7a-, and PTP-7b-induced cell lysis in A549 using LDH kit. Cells were incubated with peptide solutions of various concentrations for 20 min (A) or 60 min (B), and then assessed by the measurement of LDH released from the damaged cells. Results were normalized to 100% percentage of the total LDH released by LDH Assay Lysis Solution. Data represents the mean and SD of three independent tests.

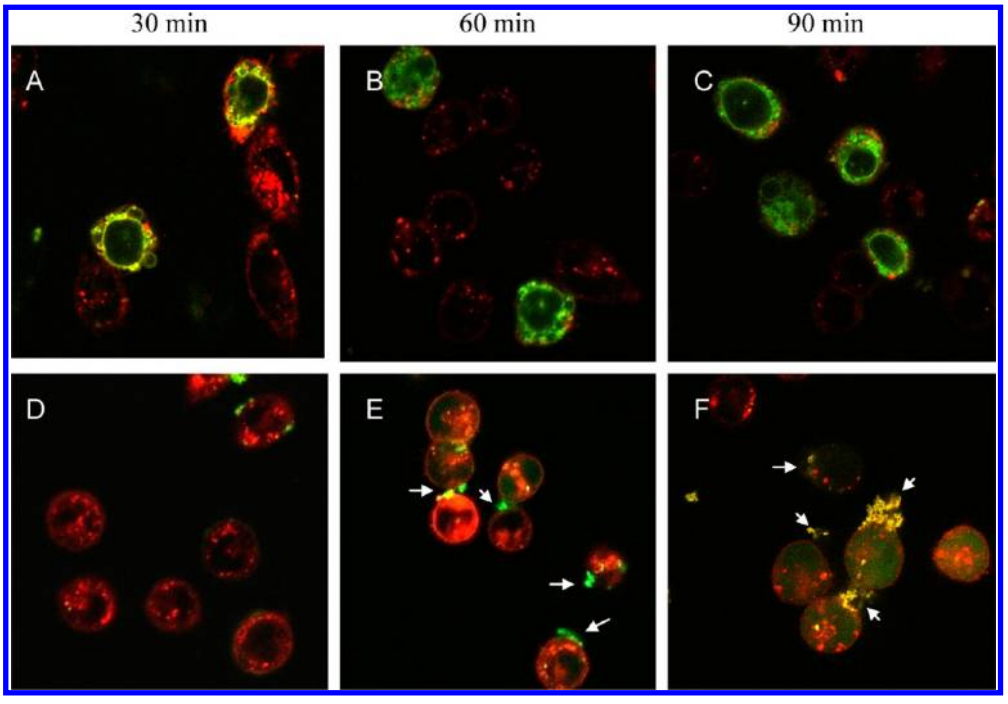

Figure 5. Kinetics of peptide interaction with A549 cells leading to cell membrane damage. Cells were labeled with 2.5 μM Di-8-ANEPPS. Experimental conditions: (A–C) cells were exposed to FITC-labeled peptide PTP-7 (10 μM) for 30 (A), 60 (B) and 90 (C) minutes; (D-F) cells were exposed to FITC-labeled peptide PTP-7b (40 μM) for 30 (D), 60 (E), and 90 (F) minutes. Formed peptide (green) or peptide/lipid (yellow) aggregates on cell membranes are indicated by arrows.

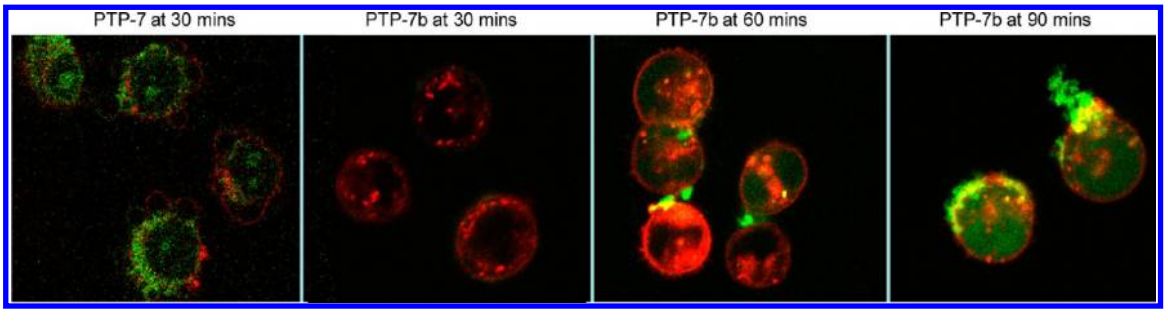

Figure 6. Comparison of FITC-labeled PTP-7- and PTP-7b-induced cells lysis on A549 cells. A549 cell membranes were labeled by Di-8-ANEPPS. Peptide concentration was fixed at 40 μM.

the incubation time passed the transition time point (>60 min). During the early phase (30–60 min) of incubation, a large amount of PTP-7b was found inside cells with intact cell membranes. Intracellular PTP-7b was evenly distributed

dx.doi.org/10.1021/bm301106p | *Biomacromolecules* 2012, 13, 3327–3333

between cytoplasm and nuclei. By contrast, although PTP-7 also entered into cells with severely damaged cell membranes, peptide PTP-7 was only found in the cytoplasm but not in the nuclei. This distinguishing peptide intracellular distribution also reflected the difference between PTP-7 and PTP-7b interaction with cell membranes, the nucleus membranes in this case.

Details of peptide-induced cell membrane damage were also studied using SEM (Figure 7). Untreated A549 cells had

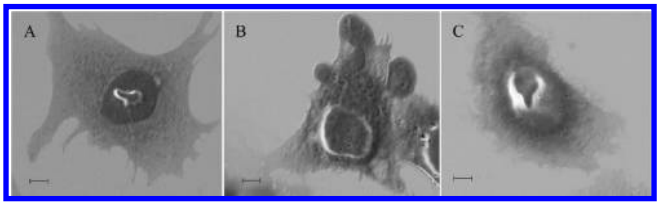

Figure 7. SEM images of A549 cells (A) treated by 10 μM peptide PTP-7 (B) and 40 μM PTP-7b (C) for 60 min. Cell samples were first fixed and then coated with gold for SEM analysis. Scale bar = 5.0 μm.

smooth cell membranes and showed a clear membrane border. Severely damaged cell membranes and small lipid vesicles were clearly seen in PTP-7-treated cells. Although PTP-7b-treated cells could keep their cell shape, the clear membrane border as seen in the untreated cells was not found. The whole cell surface was covered by fibril-like clusters. According to the results of the confocal microscopy assay (Figure 5G), these fibril-like clusters represented peptide aggregates on cell surfaces composed by either pure PTP-7b or PTP-7b/lipid mixtures.

It should be noted that PTP-7b took a long time to induce cell lysis in comparison with PTP-7 (60 min vs 10 min) (Figure 3). We compared the cell binding kinetics of PTP-7 with PTP-7b by measuring the transmembrane potential changes in cells caused by peptide binding (Figure 8). Although PTP-7b was less potent than PTP-7 because of its lower number of positive charges (Figure 8), dramatic and immediate transmembrane potential change was observed in cells treated by either peptide, indicating that significant amounts of PTP-7 and PTP-7b were attracted to and accumulated on cell surfaces quickly. This result was consistent with the fact that PTP-7b was found on cell surfaces after 30 min of incubation (Figure 5) and confirmed that peptide binding to cell membranes did not contribute to the long induction time of PTP-7b.

We found in a previous study that peptide aggregates from PTP-7b were acid sensitive and dissolved in acidic solutions completely and immediately as the imidazole group of histidine residue was protonated.[10] However, the assembling of PTP-7b into aggregates proved to be a slow process that started at 2 h and completed after 4–6 h of incubation once the solution pH was adjusted back to neutral (Figure 9). This result matched well with PTP-7b self-assembling kinetics observed on cell membranes where a continuous size increase of PTP-7b aggregates was accompanied by the disappearance of the initially formed thin peptide layer on cell surfaces (Figure 6). Therefore, it seems that migration of cell membrane bound peptides to certain places to form peptide aggregates is the limiting step and is responsible for the long induction time of PTP-7b (Figure 3). It should be pointed out that peptide nucleation on cell membranes may be through two different mechanisms: first, the aggregation is specifically nucleated on the cell surface, which involves certain agents such a receptor, a protein, or a fluctuation in cell membranes; second, the

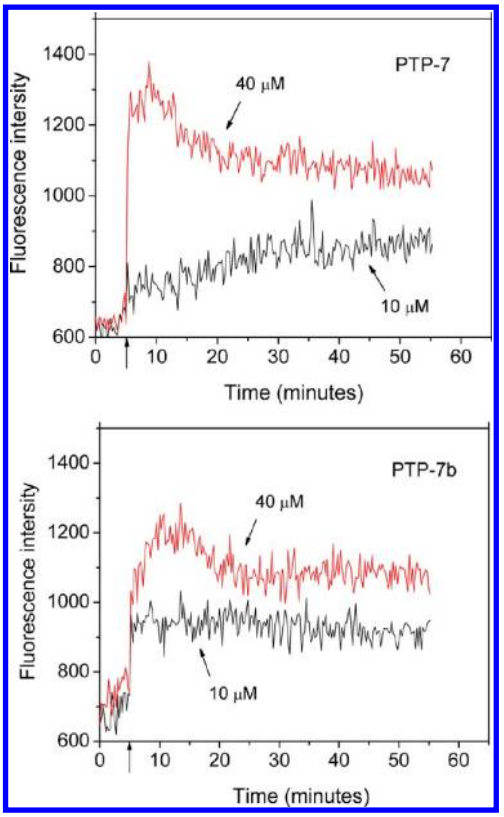

Figure 8. Comparison of PTP-7- and PTP-7b-induced transmembrane potential changes on A549 cells. Freshly trypsinized A549 cells were washed and stained with 5 μM DiSC3(5), and fluorescence intensity changes were measured after peptides were added (indicated by arrows on the *x*-axis).

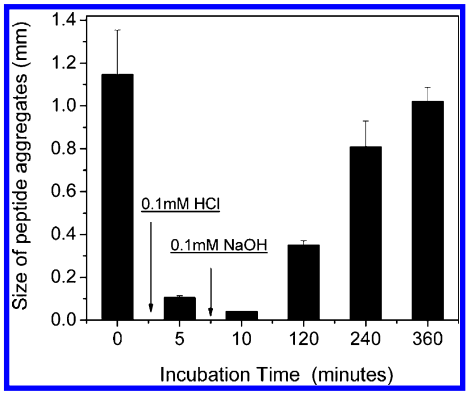

Figure 9. The pH-affected self-assembly of peptide PTP-7b. PTP-7b aggregates dissociated immediately after HCl was added and the solution was adjusted to acidic. PTP-7b reassembling into aggregates was monitored for up to 6 h after equal moles of NaOH was added to adjust the solution pH to neutral. Particle size changes of peptide aggregates were measured using a Nanosizer.

nucleation is random and occurs around centers that happen to be created first. Although we can not completely exclude the first possibility, experimental results suggest that the nucleation occurs at the place it happened first. Because PTP-7b aggregation is concentration-dependent (Figure 2), as PTP-7b binds to cell membranes and is concentrated on the cell surfaces, accelerated peptide aggregation is expected in the presence of cells. This explains the aggregation kinetic

dx.doi.org/10.1021/bm301106p | *Biomacromolecules* 2012, 13, 3327–3333

difference of PTP-7b in the absence (Figure 9) and presence (Figure 6) of cells.

In order to prove that the unusual acting mechanism of PTP-7b was directly linked to PTP-7b self-assembling on cell surfaces, we compared the dynamics of PTP-7- and PTP-7b-induced cell lysis under acidic conditions (Figure 10). The

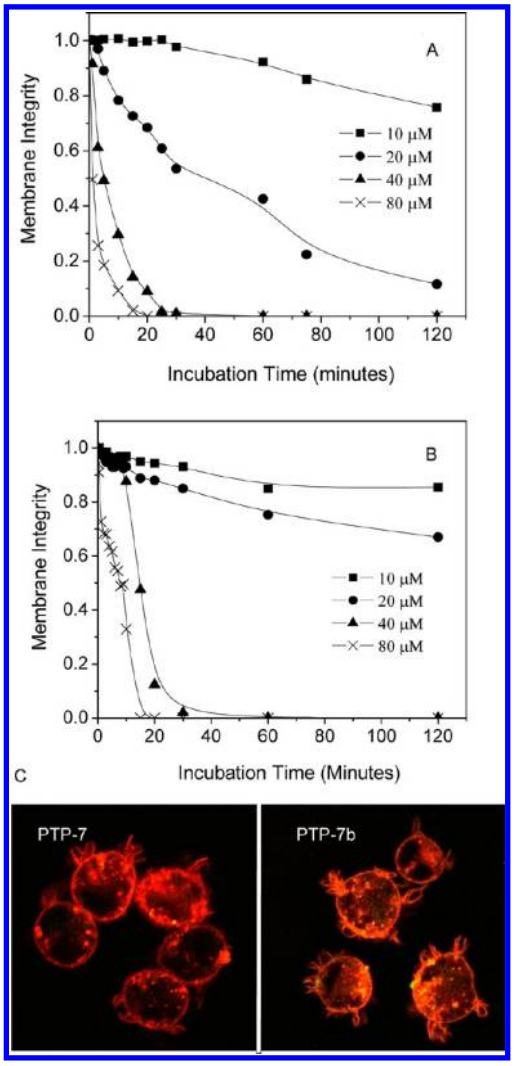

Figure 10. Dynamics of PTP-7 (A) and PTP-7b (B) induced cell membrane permeation to LIVE/DEAD dyes under acidic condition (pH = 5.5). (C) Confocal images of PTP-7 and PTP-7b induced cell membrane damages at pH = 5.5.

biphasic cell membrane lysis behaviors of PTP-7b observed at pH = 7.5 (Figure 3) was not found under acidic conditions (pH = 5.5) when PTP-7b could not self-assemble into aggregates (Figure 10B). Peptides PTP-7 and PTP-7b gave almost identical cell lysis profiles (Figure 10A,B) and followed the same mechanism, most likely a toroidal model (Figure 10C). These results provide direct evidence to support the importance of peptide self-assembly in PTP-7b-mediated cell lysis.

It is known that unlike PTP-7, peptide PTP-7b presents as an α helix in the solution.[10] A model to describe the acting mechanism of peptide PTP-7b is proposed (Figure 11). PTP-7b peptides are attracted to negatively charged cell membranes, bind to cell surfaces, and insert into the plane of cell membranes. The bound PTP-7b peptide can migrate along

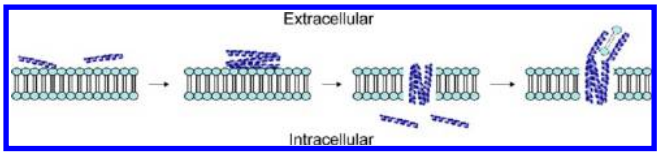

Figure 11. A proposed model for peptide PTP-7b-induced cell lysis.

the cell surface to self-assemble into aggregates at certain locations on cell membranes. As the peptide aggregates become larger, they insert deep into cell membranes and form cross membrane aggregates. Because of the difference between intracellular and extracellular environments, the intracellular parts of the PTP-7b aggregates are dissolved and release PTP-7b into the cytoplasm. In the late phase, negatively charged and polar lipid molecules in cell membranes participate in PTP-7b self-assembly on cell membranes and form exosome-like aggregates composed of a mixture of peptide and lipids. As lipid molecules are continuously extracted into the exosome-like aggregate from cell membranes, the integrity of the cell membranes is disrupted and eventually leads to a rapid cell lysis.

CONCLUSIONS

The effects of positive charges and secondary structures on peptide-cell membrane interactions have been well studied.[3−9] Self-assembly of peptides in cell membranes was reported in a very recent publication.[18] We demonstrate for the first time that peptide aggregates from peptide self-assembly can contribute significantly to cell-peptide interactions. This cell lysis mediated by peptide aggregates represents a new mechanism that cannot be described by currently available models.

Self-assembling into aggregates with defined structures is a common phenomenon for most peptides, especially at high peptide concentrations.[15−17] All peptides tend to form aggregates and may never exist as single molecules in solution.[10] In this regard, peptide self-assembly can be as important as charge and peptide secondary structure in determining the biological activity of peptides. We have reported that aggregated peptides become resistant to enzymes and have long life-spans in human plasma.[10] Therefore, our research may reveal a new and much easier way to manipulate the biological activity of therapeutic peptides for wide biomedical applications.

AUTHOR INFORMATION

Corresponding Author

*Mailing address: Department of Chemistry, Chemical Biology, and Biomedical Engineering, Stevens Institute of Technology, Castle Point on Hudson, Hoboken, NJ 07030, USA. Tel.: 201-216-5640; Fax: 201-216-8240; E-mail: jliang2@stevens.edu.

Notes

The authors declare no competing financial interest.

ACKNOWLEDGMENTS

This work was supported by NIH Grant GM081874. L.C. is a recipient of the Innovation and Entrepreneurship Doctoral Fellowship.

REFERENCES

(1) Vlieghe, P.; Lisowski, V.; Martinez, J.; Khrestchatisky, M. *Drug Discovery Today* **2010**, *15*, 40−56.

(2) Wraith, D. C. *Immunol. Lett.* **2009**, *122*, 134−136.
(3) Shai, Y. *Biopolymers* **2002**, *66*, 236−248.
(4) Bechinger, B. *Crit. Rev. Plant Sci.* **2004**, *23*, 271−292.
(5) Brogden, K. A. *Nat. Rev. Microbiol.* **2005**, *3*, 238−250.
(6) Sato, H; Feix, J. B. *Biochim. Biophys. Acta* **2006**, *1758*, 1245−1256.
(7) Hoskin, D. W.; Ramamoorthy, A. *Biochim. Biophys. Acta.* **2008**, *1778*, 357−375.
(8) Terzi, E.; Hölzemann, G.; Seelig, J. *Biochemistry* **1997**, *38*, 14845−14852.
(9) Frank, S. *Eur. J. Pharmacol.* **2009**, *625*, 190−194.
(10) Chen, L.; Tu, Z.; Voloshchuk, N.; Liang, J. F. *J. Pharm. Sci.* **2012**, *101*, 1508−15017.
(11) Zhao, X.; Zhang, S. *Macromol. Biosci.* **2007**, *7*, 13−22.
(12) Scanlon, S.; Aggeli, A. *Nano Today* **2008**, *3*, 22−30.
(13) Henriques, S. T.; Pattenden, L. K.; Aguilar, M.; Castanho, M. A. R. B. *Biophys. J.* **2008**, *95*, 1877−1889.
(14) Tu, Z.; Volk, M.; Shah, K.; Clerkin, K.; Liang, J. F. *Peptides* **2009**, *30*, 1523−1528.
(15) Subbalakshmi, C.; Manorama, S. V.; Nagaraj, R. *J. Pept. Sci.* **2012**, *18*, 283−292.
(16) Meng, Q.; Kou, Y.; Ma, X.; Liang, Y.; Guo, L.; Ni, C.; Liu, K. *Langmuir* **2012**, *28*, 5017−5022.
(17) Castelletto, V.; Cheng, G.; Hamley, I. W. *Chem. Commun. (Cambridge, U. K.)* **2011**, *47*, 12470−12472.
(18) Wadhwani, P.; Strandberg, E.; Heidenreich, N.; Bürck, J.; Fanghänel, S. *J. Am. Chem. Soc.* **2012**, *134*, 6512−6515.
(19) Terzi, E.; Hölzemann, G.; Seelig, J. *Biochemistry* **1997**, *36*, 14845−14852.